Intraparticle Diffusion in Hydrogenation of 3-Hydroxypropanal

X. Zhu and H. Hofmann
Institute of Technical Chemistry, University of Erlangen-Nürnberg, 91058 Erlangen, Germany

Strong intraparticle diffusion resistance was observed and the apparent effectiveness factors were measured for the hydrogenation of 3-hydroxypropanal (HPA) to 1,3-propanediol (PD) over $Ni/SiO_2/Al_2O_3$ catalyst pellets at 45 to 80°C and 2.60 to 5.15 MPa in a stirred reactor with a spinning basket. A mathematical model was proposed to describe the intraparticle diffusion and to estimate the effective diffusion coefficients of HPA, PD and hydrogen under reaction conditions by a maximum likelihood function of the apparent effectiveness factors of HPA and PD. The calculated concentration distributions of HPA, PD and hydrogen in catalyst particles reveal an excess of hydrogen at 80°C and higher temperatures, but an excess of HPA at 45°C. It results in a weak dependence of the consumption formation rate of HPA and PD on the partial pressure of hydrogen at high temperature.

Introduction

The heterogeneous catalytic hydrogenation of 3-hydroxypropanal (HPA) formed by the hydration of the acrolein (Ac) is an important process to produce 1,3-propanediol (PD), a potentially attractive monomer for polymers (Arntz et al., 1991; Unruh et al., 1992). The process can be carried out in a slurry reactor or a trickle-bed reactor. Catalyst pellets instead of powder have to be used to overcome difficulties caused by the separation of the catalyst from the liquid phase in a slurry reactor or to avoid a large pressure drop in a trickle-bed reactor. In this case the intraparticle diffusion resistance must be considered to model the hydrogenation of HPA.

Investigations of intraparticle diffusion in the hydrogenation of α-methylstyrene over $Pd-Al_2O_3$ (Satterfield et al., 1968, 1969), of crotonaldehyde over $Pd/\gamma-Al_2O_3$ (Kenney and Sedriks, 1972), of isopropanol over Raney-Ni (Lemcoff and Jameson, 1975), of styrene over $0.5\%Pd/Al_2O_3$ (Kawakami et al., 1976), of glucose and butynediol over Ni/SiO_2 (Turek et al., 1983; Turek and Winter, 1990) have been reported in the literature. However, these studies only involved the intraparticle diffusion of hydrogen because it was thought to be the rate-controlling step. The tortuosity factors of hydrogen in the literature vary from 1.6 to 7.5, depending on experimental conditions. The intraparticle diffusion in hydrogenation of HPA with $Ni/SiO_2/Al_2O_3$ cylindrical catalyst particles has not yet been investigated. It is the purpose of this article to measure or estimate the effective diffusion coefficients of HPA, PD, and hydrogen under reaction conditions.

Several methods have been used to measure the effective diffusion coefficient, for instance, the classic method of Wicke and Kallenbach (1941), the dynamical adsorption method of Ruthven (1984) and Shah and Ruthven (1977), the effectiveness factor-Thiele modulus method of Turek et al. (1983) and Haag et al. (1981), and the NMR pulse-field gradient method of Pfeifer (1976). Except for the effectiveness factor-Thiele modulus approach, these methods cannot be easily applied to measure the effective diffusion coefficient under reaction conditions. The effectiveness factor-Thiele modulus approach has been applied only to a simplified system (for example, to a first-order reaction and large Thiele-modulus, e.g., greater than 3). An alternate method is introduced in this article to solve this complicated problem. In principle the effective diffusion coefficients can be estimated by a maximum-likelihood function of apparent effectiveness factors calculated by either experimental results of intrinsic and effective kinetics or a mathematical model. The intrinsic kinetics of the hydrogenation of HPA has been studied by Zhu (1995) and Zhu et al. (1996b). For measurements of apparent effectiveness factor the hydrogenation of HPA was carried out over $Ni/SiO_2/Al_2O_3$ catalyst pellets in a spinning-basket reactor under conditions that did not include the

Correspondence concerning this article should be addressed to H. Hofmann.

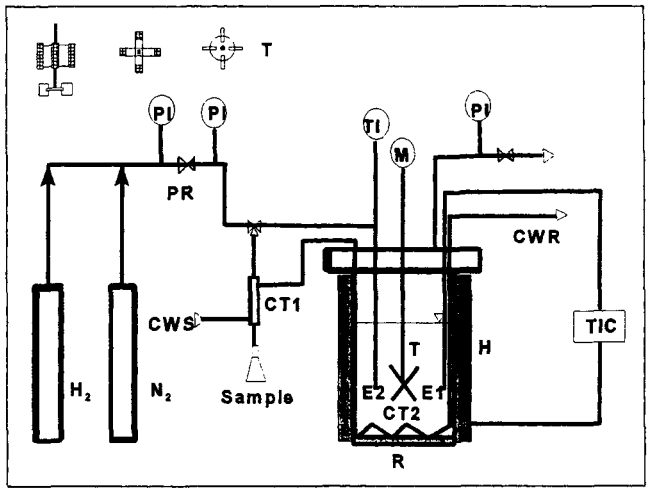

Figure 1. Experimental equipment.

CT1, CT2: cooling tubes 1 and 2; CWR: cooling water return; CWS: cooling water supply; E1, E2: thermocouples 1 and 2; H: electrical heater; M: motor; PI: pressure indicator; R: autoclave; T: turbine impeller; TI: temperature indicator; TIC: temperature indicator controller.

external mass-transfer resistance. At this condition the concentration–time profiles of HPA and PD were measured at different temperatures and pressures. On the other hand, a mathematical model describing the apparent effectiveness factors must be developed before the effective diffusion coefficients can be estimated by a multiresponse regression method.

Experimental

Equipment

The experimental apparatus is shown in Figure 1. It consists of a 2-L spinning-basket reactor (R) with the basket fixed on the shaft 1 cm above the four-blade turbine impeller (T) driven by a variable speed motor (M), a temperature control system (two thermocouples E1 and E2, a cooling tube CT2, an electric heater H, an electronic temperature controller TIC), and a pressure control system (a pressure reducer PR and three pressure indicators PI).

Materials

The catalyst pellets were supplied by Süd-Chemie AG. Their physical and chemical properties were measured and are shown in Table 1. A 10 wt. % aqueous HPA solution was used. Its composition was reported by Zhu (1994). Linde Co. supplied the 99.99 wt. % hydrogen.

Experimental procedure

In an experiment 20 g catalyst pellets were placed in the basket and then the basket was fixed to the shaft. A 1.0-L aqueous HPA solution was fed into the autoclave. The experimental setup was flushed with nitrogen after the autoclave was sealed. The autoclave was heated to the desired temperature by stirring, and then purged with hydrogen without stirring, and finally pressurized to the desired pressure. Before the motor was started again, the first sample was taken. Hydrogenation was carried out at constant temperature and pressure. The samples were taken within a certain reaction time interval after purging the sample tube. To avoid errors caused by the change of solution volume, the total amount of samples was less than 20 mL. Each sample was analyzed by gas chromatography (DANI 8521-A with FED 651.1).

Table 1. Chemical Composition and Physical Properties of the Catalyst Pellets

Chemical Composition		Physical Properties	
Component	wt. %	Form	Cylindric
Ni	50–52	Size	Φ 0.8×3–8 mm
SiO_2	25	Bulk density	600 kg/m^3
Al_2O_3	10	Particle density	1,430 kg/m^3
Others	13–15	Surface area	209 m^2/g
		Average diameter of (nm)	
		Micropores	0.8
		Mesopores	3.9

Results and Discussion

Experimental results

The gas–liquid–solid mass-transfer resistance can be ignored at an agitation speed higher than 400 L/min if the other reaction conditions are as follows: amount of catalyst, 20 g/L; temperature, ≤ 85°C; and pressure, ≥ 2.5 MPa. This has been verified by increasing the agitation speed to 500 L/min without any effect on the reaction process.

Besides two homogeneous side reactions (Eqs. B and C), a heterogeneous catalytic main reaction and a side reaction occur simultaneously in the hydrogenation of HPA over $Ni/SiO_2/Al_2O_3$ catalyst pellets (Zhu, 1995; Zhu et al., 1996a). They are expressed as:

Main reaction

$$\mathrm{HPA} + \mathrm{H_2} \xrightarrow{\text{cat.}} \mathrm{PD}. \qquad \text{(A)}$$

Side reactions

$$\mathrm{HPA} + \mathrm{PD} \xrightarrow{\text{cat.}} \mathrm{Acetal} + \mathrm{H_2O} \qquad \text{(B)}$$

$$\mathrm{HPA} \rightleftharpoons \mathrm{Ac} + \mathrm{H_2O} \qquad \text{(C)}$$

$$\mathrm{HPA} + \mathrm{Ac} \rightarrow \text{4-Oxa-1.7-Heptandial}. \qquad \text{(D)}$$

The concentration-time profiles of reactants and products at different temperatures and pressures were measured. Values of apparent effectiveness factors η_i of component i were determined according to the definition (Eq. 1)

$$\eta_i = \frac{R_{ei}(C,T)}{R_i(C,T)} \qquad (1)$$

in the following way: the concentration C_i (i = HPA and PD) was at first expressed as a power-series function of the reaction time (t) $C_{1,i} = \Sigma a_{ij} t^j$ ($j = 0, \ldots, 4$), whose coefficients were determined by linear regression. Then the apparent rates of formation R_{ei} (i = HPA and PD) were calculated by abstracting the contribution (calculated by a combination of

Eqs. 3 to 7, e.g., $r_3 - r_{-3} + r_4$ is the contribution of side reactions C and D to the rate of formation of the component HPA) of homogeneous side reactions from the derivative of the concentration C_i/C_k with respect to time t, where C_k is the catalyst concentration.

The intrinsic rates of formation R_i (i = HPA and PD) were calculated at the same reaction conditions by Eqs. 2 combined with the intrinsic kinetic model (Eqs. 3 to 7)

$$R_{\mathrm{HPA}} = -\frac{dC_{\mathrm{HPA}}}{C_k dt} = r_1 + r_2 \qquad R_{\mathrm{PD}} = \frac{dC_{\mathrm{PD}}}{C_k dt} = r_1 - r_2. \quad (2)$$

The rate r_j of the reactions j ($j = 1, 2, 3, -3, 4$) can be written as

$$r_1 = \frac{k_1 P C_{\mathrm{HPA}}}{H\left(1 + \sqrt{K_1 \frac{P}{H}} + K_2 C_{\mathrm{HPA}}\right)^3} \quad (3)$$

$$r_2 = \frac{k_2 C_{\mathrm{PD}} C_{\mathrm{HPA}}}{1 + \sqrt{K_1 \frac{P}{H}} + K_2 C_{\mathrm{HPA}}} \quad (4)$$

$$r_3 = k_3 C_{\mathrm{HPA}} \qquad r_{-3} = k_{-3} C_{Ac} \quad (5)$$

$$r_4 = k_4 C_{Ac} C_{\mathrm{HPA}} \quad (6)$$

$$k_j = k_{oj} \exp\left(-\frac{\Delta E_j}{RT}\right) \qquad K_i = K_{oi} \exp\left(-\frac{\Delta H_i}{RT}\right), \quad (7)$$

where k_j ($j = 1, 2, 3, -3, 4$) are the intrinsic reaction-rate constants; K_i ($i = 1\text{-}H_2$, 2-HPA) are the adsorption equilibrium constants of H_2 and HPA; C_i (i = HPA, PD, Ac) are the concentrations of component i. The preexponential factors K_{oi} and k_{oj}, the activation energy ΔE_j of reaction j, and the desorption enthalpy ΔH_i of component i are shown in Table 2. They were estimated by minimizing the sum of the squared differences between the measured and calculated concentrations of HPA and PD. Besides the accurate measurements of the concentration–time profiles, a good intrinsic kinetic model is very important for obtaining good values of the apparent effectiveness factors (for details, see Zhu et al., 1996a).

Table 2. Estimated Parameters of the Intrinsic Kinetics

i/j	k_{0j} L²/mol·s·g	K_{oi} L/mol	ΔE_j kJ/mol	ΔH_i kJ/mol
1	1.545×10^{8}	1.785×10^{4}	55.589	−13.844
2	6.110×10^{11}	0.6988	104.06	4.046
3	2.278×10^{9}	—	93.390	—
−3	6.739×10^{3}	—	53.256	—
4	2.207×10^{21}	—	173.68	—

Source: Zhu, 1995; Zhu et al., 1996a.

The measured apparent effectiveness factors of HPA and PD at different temperatures and pressures are shown in Figures 2 and 3. Intraparticle diffusion resistance is strong in the hydrogenation of HPA over the catalyst pellets because the apparent effectiveness factors are much less than 1. Furthermore, the apparent effectiveness factors of HPA, PD, and hydrogen are different from each other and strongly dependent on the temperature and the concentrations of HPA and hydrogen. They decrease when the temperature increases from 60°C to 80°C. However, a positive effect of the temperature was also observed in the range of the HPA-concentration, 1.25–1.36 mol/L, between 45°C and 60°C (see Figure 3). This can be explained by a simplified Eq. 8

$$\eta = \eta(c_s, k, D_e); \qquad \frac{d\eta}{dT} = \frac{\partial \eta}{\partial D_e}\frac{dD_e}{dT} + \frac{\partial \eta}{\partial k}\frac{dk}{dT}, \quad (8)$$

where k is the reaction rate constant and D_e the effective diffusion coefficient. In general

$$\frac{\partial \eta}{\partial D_e} > 0 > \frac{\partial \eta}{\partial k}; \qquad 0 < \frac{dD_e}{dT} < \frac{dk}{dT}. \quad (9)$$

It is therefore possible that the value of the derivative of the apparent effectiveness factor with respect to the temperature

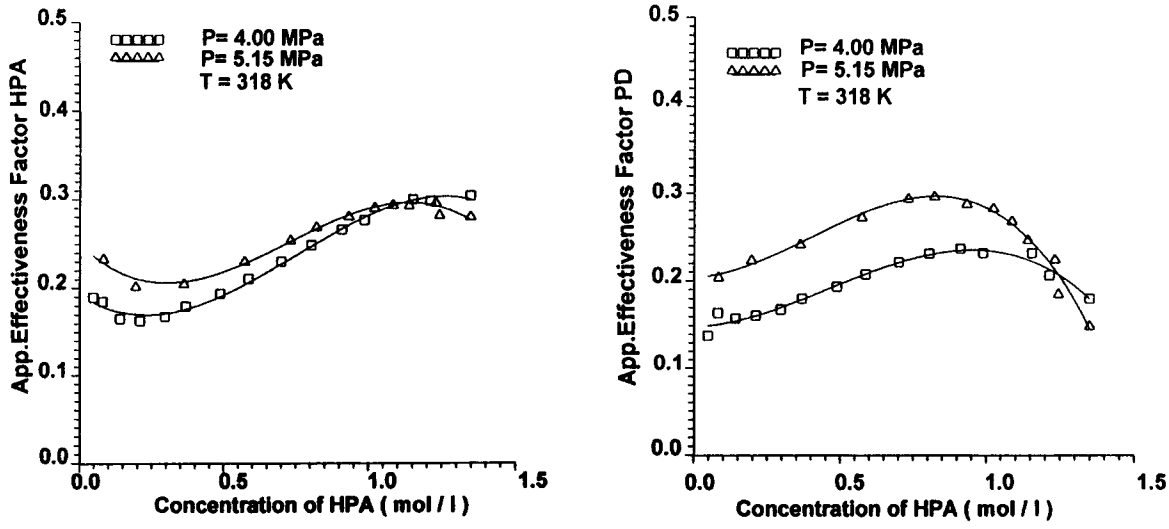

Figure 2. Apparent effectiveness factors of HPA and PD at different pressures.

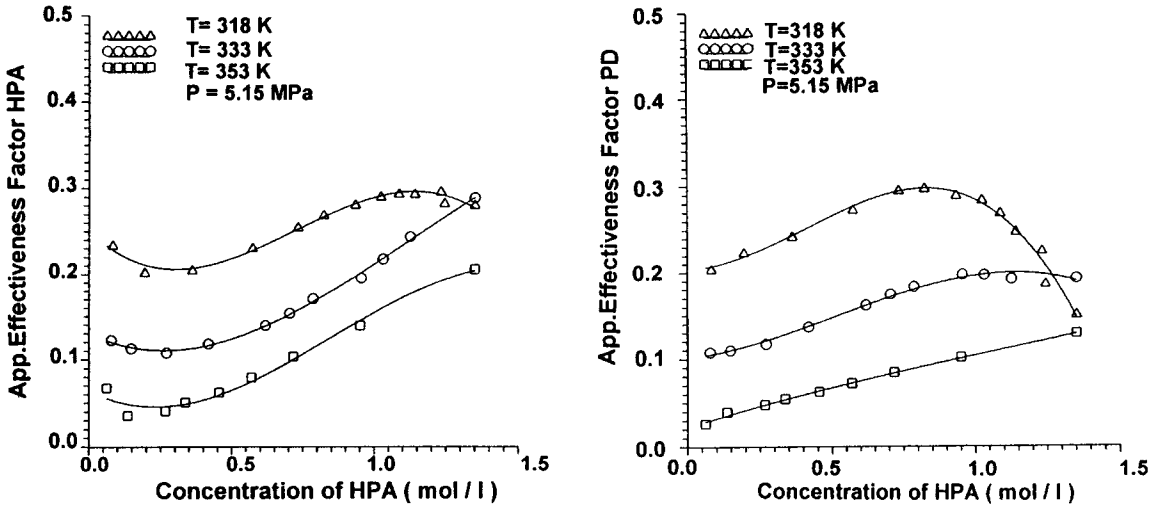

Figure 3. Apparent effectiveness factors of HPA and PD at different temperatures.

is positive, that is, the apparent effectiveness factor increases with temperature.

Figure 2 shows a positive effect of the pressure of hydrogen on the apparent effectiveness factors of HPA and PD in a wide range of HPA-concentration. At 45°C the higher the hydrogen pressure is, the greater the value of the apparent effectiveness factors. The increase of PD's apparent effectiveness factor with increasing hydrogen pressure is greater than that of HPA. So a high PD selectivity of catalyst particles is reached at high hydrogen pressure. However, the positive effect of hydrogen pressure becomes less if the temperature increases, as shown in Figure 4. The difference in the rate of formation of HPA and PD is smaller at 60°C than at 45°C while the hydrogen pressure increases from 4.00 to 5.15 PMa.

The complex effects of HPA and hydrogen concentrations on the apparent effectiveness factor may be explained by the intrinsic kinetics for hydrogenation of HPA and the intraparticle diffusion in the catalyst particles. In a simplified form of Eq. 2 (power law) the rates of HPA and hydrogen consumption are proportional to $C_{HPA}^{n1}P^{n2}$, but the rates of diffusion are proportional only to C_{HPA} or P. So the apparent effectiveness factor increases with hydrogen pressure or HPA concentration if $n1 < 0$ and $n2 < 0$, otherwise the reverse is true. In other words, whether the apparent effectiveness factor increases with the concentration of HPA and hydrogen depends on the values of $n1$ and $n2$. In the hydrogenation of HPA the values of $n1$ and $n2$ may vary from negative to positive.

With respect to intraparticle diffusion, hydrogen is in excess in the catalyst pellets at high temperatures (described in the following sections). Due to the increase in the hydrogen concentration at elevated pressure, the reaction rate of HPA speeds up in catalyst particles. However, the apparent effectiveness factors would be decreased. The product of the reaction rate and the apparent effectiveness factor is therefore only weakly dependent on the hydrogen pressure.

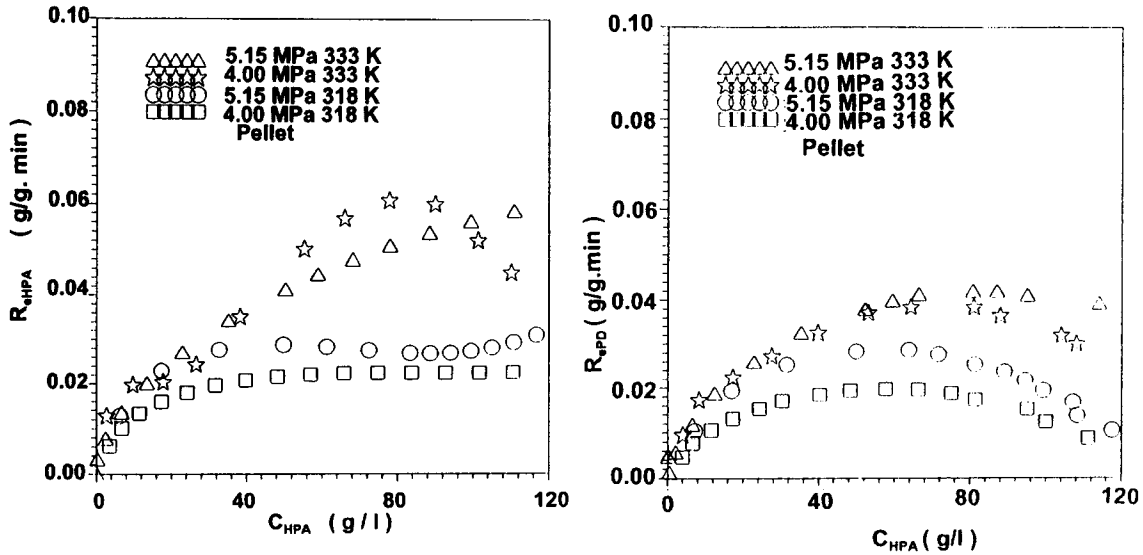

Figure 4. Effect of hydrogen pressure on the rates of consumption or formation of HPA and PD at different temperatures.

The difference in apparent effectiveness factors between HPA and PD seems to be the result of side reactions.

Since the apparent effectiveness factor is not a constant for a complex reaction system, effective kinetic models such as power-law or hyperbolic models, whose parameters are estimated by a regression in the data measured with catalyst particles, are in principle empirical, as they are based on a constant apparent effectiveness factor. Such an effective kinetic model is not reliable for processing scale-up, as its parameters may vary with a change in catalyst particle size or reaction conditions. Instead, the method described by Zhu (1995) and Zhu et al. (1996a), where the effective diffusion coefficients are used as a model parameter, should be applied to model the reaction processes with strong intraparticle diffusion.

Model for apparent effectiveness factor

When the catalyst particles in the reaction system do not differ from each other, the apparent effectiveness factors η_i of component i can be calculated by the apparent effectiveness factors for one catalyst particle, defined as

$$\eta_i = \frac{\iiint_{V_p} R_i(C_{H_2}, C_{HPA}, C_{PD})\, dV}{V_p R_i(C_{H_2,s}, C_{HPA,s}, C_{PD,s})} \qquad i = H_2, \text{HPA, PD,} \tag{10}$$

where V_p is the volume of a catalyst particle; and C_i and $C_{i,s}$ are the concentrations of component i ($i = H_2$, HPA, PD) in the catalyst particle and on its external surface, respectively.

The concentration C_i in the catalyst particles can be calculated by solving the differential equations (a diffusion equation with reactions)

$$D_{ei}\left(\frac{d^2C_i}{dr^2} + \frac{1}{r}\frac{dC_i}{dr}\right) = \rho_p R_i \qquad i = H_2, \text{HPA, PD,} \tag{11}$$

with boundary conditions

$$\left.\frac{dC_i}{dr}\right|_{r=0} = 0 \qquad C_i|_{r=R_p} = C_{i,s}. \tag{12}$$

Equations 11 and 12 can be derived by the mass balance of a cylindric catalyst particle, assuming that mass transfer through the external surface at both ends of the cylindric particle and the homogeneous side reactions in catalyst particles are negligible. If the apparent effectiveness factor is less than 0.35, this simplification causes an error of approximately 2% for the catalyst particle size listed in Table 1. The concentration $C_{i,s}$ on the external surface of the catalyst pellets can be replaced by the concentration in the liquid phase if the external mass transfer resistance is negligible.

Numerical solution

Since the equations that describe the reaction rates are nonlinear, one cannot obtain an analytical solution of the diffusion equations (Eq. 11). However, Eqs. 11 and 13 can be transformed by differentiation

$$\frac{d^2u_i}{d\rho^2} = \frac{1}{h^2}(u_{i,j+1} - 2u_{i,j} + u_{i,j-1})$$

$$\frac{1}{\rho}\frac{du_i}{d\rho} = \frac{1}{2jh^2}(u_{i,j+1} - u_{i,j-1})$$

$$i = H_2, \text{HPA, PD;} \qquad j = 1, 2, 3, \ldots, n \tag{13}$$

into algebraic equations

$$\boldsymbol{BU} - \boldsymbol{F} = \boldsymbol{0}, \tag{14}$$

where

$$\boldsymbol{F}_i = \left(f_{i1}, f_{i2}, \ldots, f_{in-1} - 1 - \frac{1}{2(n-2)}\right)^\tau$$

$$\boldsymbol{U}_i = (u_{i1}, u_{i2}, \ldots, u_{in-1})^\tau \qquad i = H_2, \text{HPA, PD}$$

$$u_{ij} = \frac{C_{ij}}{C_{is}} \qquad \rho = \frac{r}{R_p} \qquad f_{ij} = \frac{h^2 R_p^2 \rho_p R_{ij}}{D_{ei} C_{is}} \tag{15}$$

$$\boldsymbol{B} = \begin{pmatrix} \boldsymbol{A} & 0 & 0 \\ 0 & \boldsymbol{A} & 0 \\ 0 & 0 & -\boldsymbol{A} \end{pmatrix}$$

$$\boldsymbol{U} = (\boldsymbol{U}_1, \boldsymbol{U}_2, \boldsymbol{U}_3)^\tau \qquad \boldsymbol{F} = (\boldsymbol{F}_1, \boldsymbol{F}_2, \boldsymbol{F}_3)^\tau \tag{16}$$

$$\begin{matrix}
-1.5 & 1+\frac{1}{2} & 0 & \cdot & 0 & 0 & 0 & 0 & 0 \\
1-\frac{1}{4} & -2 & 1+\frac{1}{4} & 0 & \cdot & \cdot & \cdot & \cdot & \cdot \\
0 & 1-\frac{1}{6} & -2 & 1+\frac{1}{4} & 0 & \cdot & \cdot & \cdot & \cdot \\
0 & 0 & \cdot & -2 & \cdot & 0 & \cdot & \cdot & \cdot \\
0 & 0 & \cdot & 0 & 1-\frac{1}{2j} & -2 & 1+\frac{1}{2j} & 0 & \cdot \\
0 & 0 & \cdot & \cdot & \cdot & 0 & \cdot & \cdot & \cdot \\
0 & 0 & 0 & 0 & 0 & 0 & \cdot & 0 & 1-\frac{1}{2(n-1)}
\end{matrix} \tag{17}$$

The numerical solution of Eq. 14 can be obtained by the following iteration

$$U_{m+1} = U_m - \left(B - \frac{\partial F_m}{\partial U_m} \right)^{-1} (BU_m - F_m) \qquad (18)$$

until the sum of the absolute error between U_{m+1} and U_m is less than 0.001.

Estimate of the effective diffusion coefficients

Effective diffusion coefficients of HPA, PD, and hydrogen were estimated by minimizing the objective function F

$$F = \sum_{i=2}^{3} (\eta_{i,e} - \eta_i)^T (\eta_{i,e} - \eta_i)$$

$$= (\eta_{i1,e}, \eta_{i2,e}, \ldots, \eta_{iM,e})^T \qquad \eta_i = (\eta_{i1}, \eta_{i2}, \ldots, \eta_{iL}, \ldots, r)$$

$$\eta_{iL} = \frac{2}{R_i(C_{Ls})} \int_0^1 R_i(C_L) \rho \, d\rho \qquad i = 2, 3,$$

$$L = 1, 2, 3, \ldots, M \qquad (19)$$

$$C_1 = (C_{H_2}, C_{HPA}, C_{PD})^T$$

$$C_{Ls} = (C_{H_2,s}, C_{HPA,s}, C_{PD,s})^T, \qquad (20)$$

which can be derived from the maximum likelihood function of η_{iL} if the variables η_{iL} are statistically uncorrelated and their probability distributions are Gauss distributions with the same standard deviation. Values of the apparent effectiveness factors η_{iL} for component i (i = 2-HPA, 3-PD) were computed by the numerical integration of Eq. 18 combined with Eqs. 14 and a second-order Runge-Kutta method. A gradient method was used to minimize the objective function F.

Table 3. Effective Diffusion Coefficients and Their Confidence Intervals (r = 95%)

T (K)	P (MPa)	$D_{eH2} \times 10^5$ (cm^2/s)	$D_{eHPA_2} \times 10^6$ (cm^2/s)	$D_{ePD} \times 10^6$ (cm^2/s)
318	4.00	1.72±0.05	2.78±0.82	2.56±3.45
318	5.15	1.50±0.03	1.63±0.33	1.53±0.89
333	4.00	2.20±0.02	1.14±0.27	1.08±1.36
333	5.15	1.33±0.02	1.14±0.20	1.11±1.67
353	5.15	4.30	0.75	0.40

The effective diffusion coefficients were estimated, respectively, at different temperatures and pressures to avoid difficulties in calculation. The linearized confidence intervals ΔD_{el} were calculated by where t_α is a value of the t-distribution with a degree of freedom of 3 and $3n$ when $\alpha = 0.05$:

$$\Delta D_{el} = t_\alpha \sqrt{\frac{d_{LL} F}{(3n-1)}} \qquad L = H_2, \text{HPA, PD} \qquad (21)$$

$$D = [d_{ij}] = [J \, J^T]^{-1} \qquad i = H_2, \text{HPA, PD};$$

$$j = H_2, \text{HPA, PD} \qquad (22)$$

$$J = [J_{H_2}, J_{HPA}, J_{PD}]^T \qquad J_i = [Ji_{mL}] n \times 3$$

$$Ji_{mL} = \frac{\partial \eta_{im}}{\partial D_{el}} \qquad i = H_2, \text{HPA,PD}; \qquad m = 1, 2, \ldots, n,$$

$$l = H_2, \text{HPA,P}. \qquad (23)$$

All calculations were carried out by a Fortran program that we developed. The estimated effective diffusion coefficients and their linearized confidence intervals are given in Table 3 and partly represented in Figure 5.

The temperature has an obvious effect on the effective diffusion coefficients. The influence of pressure is, however, relatively weak, depending on the temperature. It can be ne-

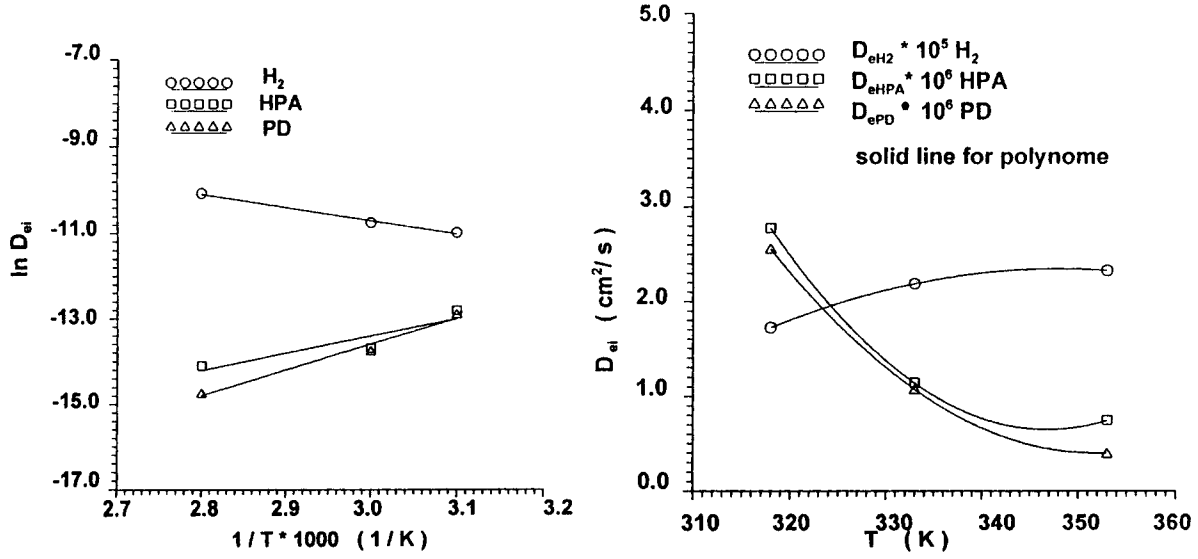

Figure 5. Effect of temperature on the effective diffusion coefficients of H_2, HPA, and PD.

A: solid line for $D_{ei} = D_{eio}(-\Delta E_i/RT)$; B: solid line for $D_{ie} = a_0 + a_1 T + a_2 T^2 + \cdots$.

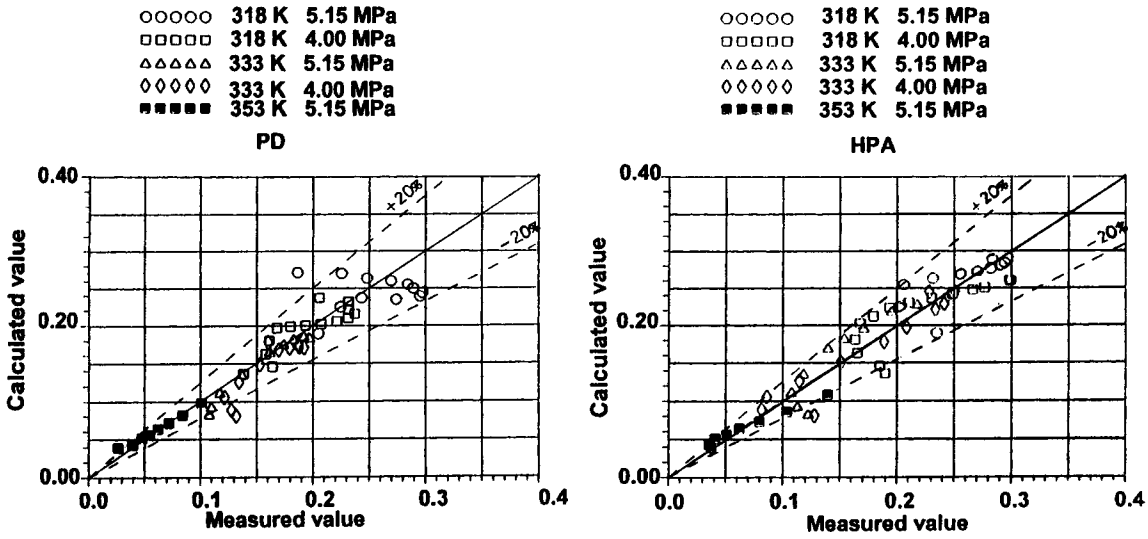

Figure 6. Apparent effectiveness factors: measured vs. calculated values of HPA and PD.

glected at 60°C. The effective diffusion coefficient of hydrogen is nearly proportional to the temperature. For HPA and PD it decreases with increasing temperature. Strong surface diffusion may result in such a temperature dependence of the effective diffusion coefficient on HPA and PD (Kärger and Ruthven, 1986). The surface diffusion of PD occurs only on the inlet catalyst surfaces, since the term of the propanediol adsorption on active sites play only a very small role in the intrinsic kinetic model (Zhu, 1995; Zhu et al., 1996a).

The large confidence intervals of the effective diffusion coefficient for PD cannot be easily reduced since the rates of formation are not sensitive to the concentration of PD. The sensitivity of rates of formation to the concentration of reactants is less if the reactants are in excess in the catalyst particles. Thus, the excess of reactants in catalyst particles should be avoided to obtain a good estimate of the effective diffusions coefficients.

The model with the estimated effective diffusion coefficients was applied to compute and predict the apparent effectiveness factors of HPA, PD, and hydrogen. Figure 6 shows that relative errors in the calculated values when compared to the experimental values are less than 20% (except for a few points). Nevertheless, the results are much better than those obtained by other methods. Hence this method is suitable to estimate the effective diffusion coefficients of hydrogen, HPA, and PD in the hydrogenation of an aqueous HPA-solution.

To determine the component that controls intraparticle diffusion, that is, which reactant is consumed fastest during diffusion from the external surface to the central part of the catalyst particles, the concentration distributions of HPA, PD, and hydrogen in the catalyst particles were computed at different temperatures and pressures. The results are shown in Figures 7, 8, and 9 at different surface concentrations, C_s, on

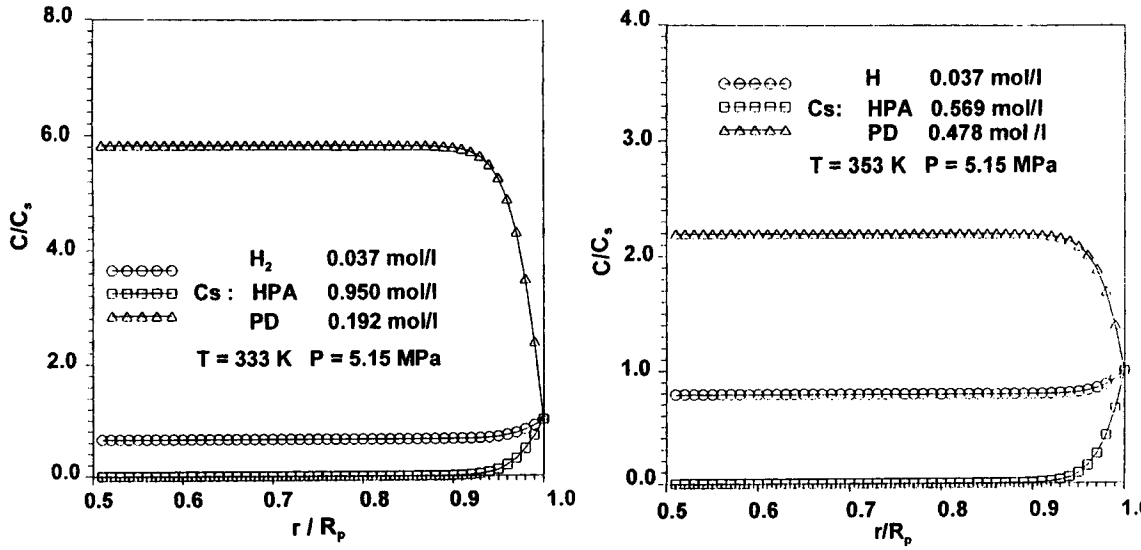

Figure 7. Profiles of H_2, HPA and PD in a cylindrical catalyst particle at different surface concentrations on the outside of the particle (80°C and 4.00 MPa or 5.15 MPa).

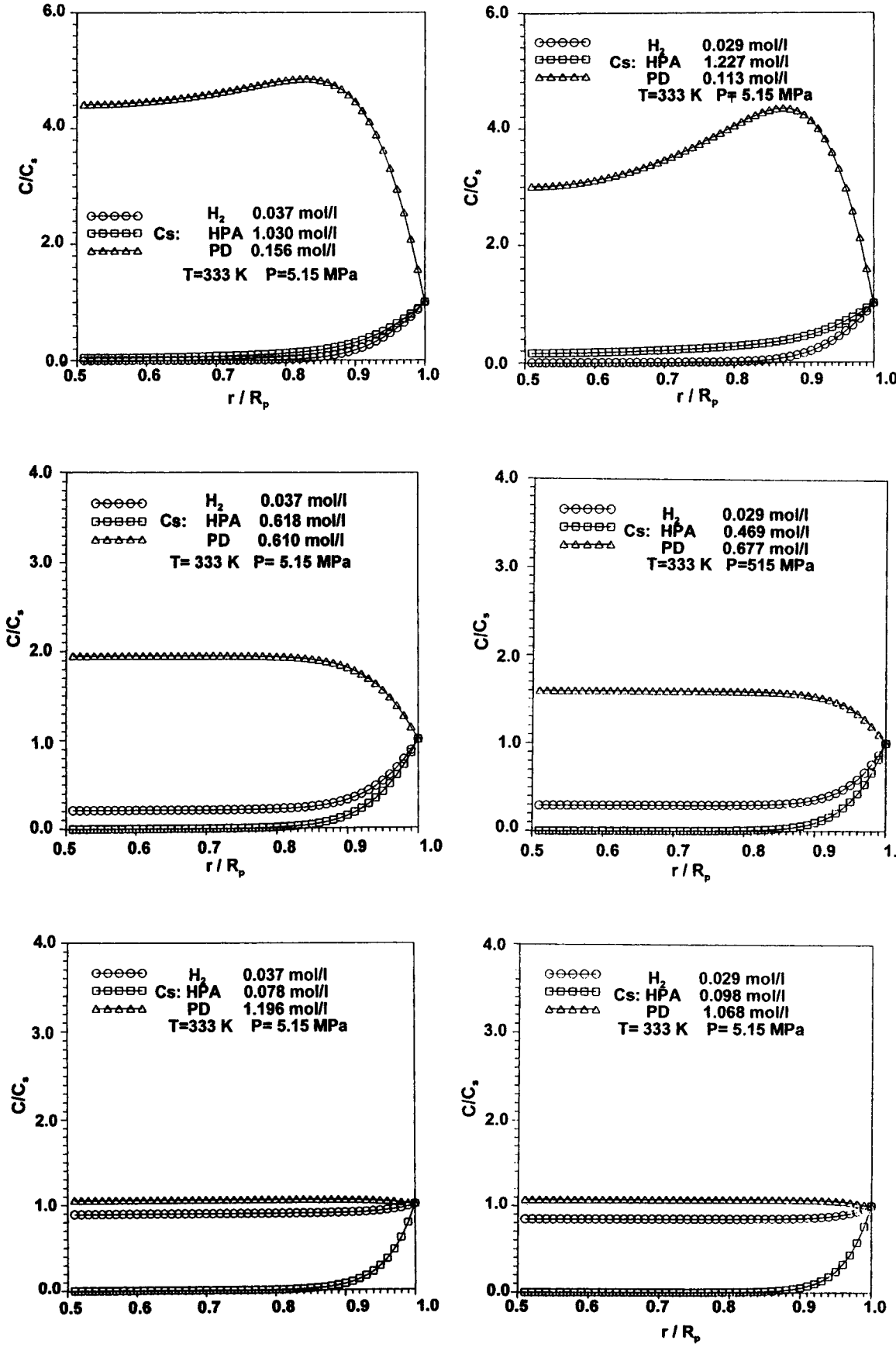

Figure 8. Concentration profiles of H_2, HPA and PD in a cylindrical catalyst particle at different surface concentrations on the outside of the particle (333 K and 4.00 or 5.15 MPa).

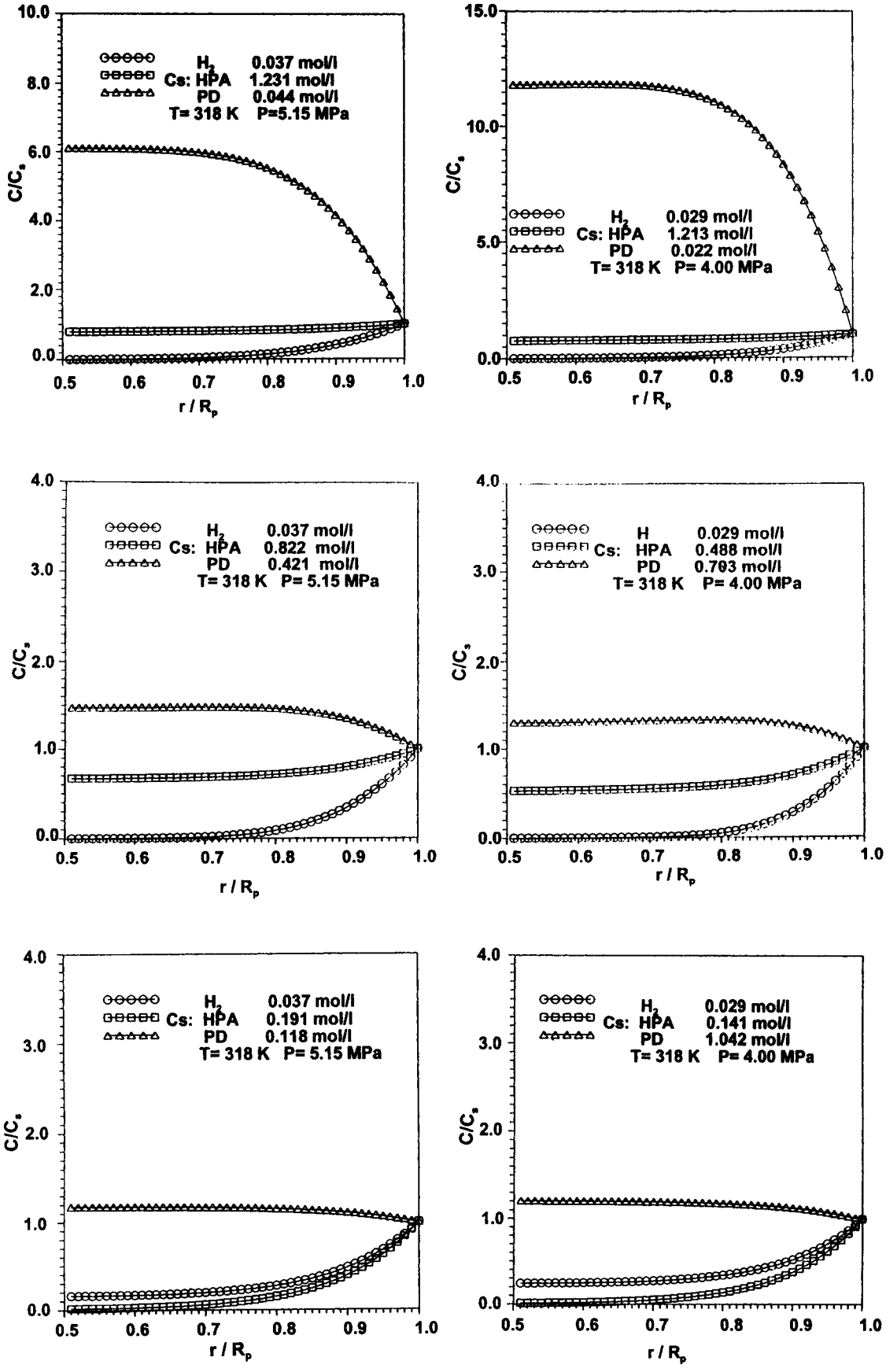

Figure 9. Concentration profiles of H_2, HPA and PD in a cylindrical catalyst particle at different surface concentrations on the outside of the particle (318 K and 4.00 or 5.15 MPa).

the catalyst particles. C_s varies with the reaction time; the longer the reaction time, the lower the surface concentration of HPA and the higher the surface concentration of PD. Figure 7 shows that the concentration of HPA decreases rapidly at 80°C from the surface concentration, C_s, to zero in the middle of the particle. At this temperature, excessive hydrogen appeared in the particle even at the start of the reaction. However, this excess disappeared as the temperature increased, as shown in Figures 8 and 9, unless a high conversion of HPA was reached. 3-Hydroxypropanal became excessive at 45°C at a lower degree of HPA conversion. No reactant is in excess at 60°C unless the conversion of HPA reaches a high value.

The results in Figures 7, 8, and 9 indicate that either hydrogen or HPA or both of them can limit the hydrogenation rate of HPA, depending on the reaction conditions and degree of conversion of HPA or the reaction time. If the degree of conversion of HPA is low and its concentration in the liquid phase is high, one can assume that HPA is in excess in the catalyst particles.

Because of the strong intraparticle diffusion resistance the catalyst particles are not completely utilized. The utilization efficiency of the catalyst particles is about 50% at 45°C, but only 20% at 80°C. At higher temperatures, the effective diffusion coefficients of HPA and PD are much lower than their diffusivity (Zhu, 1995). This may result from a microporous diameter that is too small (its average value is 0.86 nm), which is nearly as large as the molecular diameter of HPA and PD (ca. 0.82 nm and 0.84 nm, respectively). To increase the apparent effectiveness factors of HPA and PD, one should use small catalyst particles or enlarge the catalyst microporous diameter.

Conclusion

A strong intraparticle diffusion resistance, which results in a 73–95% decrease in the consumption formation rates of HPA and PD, was observed in the hydrogenation of 10 wt. % aqueous solution of HPA over $Ni/SiO_2/Al_2O_3$ catalyst pellets at 45 to 80°C and 2.60 to 5.15 MPa. The apparent effectiveness factors measured by experiments or calculated by the mathematical model were used to describe this resistance. Because of side reactions, the apparent effectiveness factors of HPA and PD differ from each other. Their dependence on the temperatures and concentrations of HPA and hydrogen is complex. In general, greater apparent effectiveness factors are obtained at lower temperatures and reactant concentrations, but also at higher temperatures and reactant concentrations.

By using a multiresponse regression method to minimize the deviation in the calculated values of the apparent effectiveness factors from their measured values, the effective diffusion coefficients of HPA, PD, and hydrogen have been estimated. The calculated apparent effectiveness factors usually show a less than 20% relative error in comparison to their measured values. This method allows us to obtain the effective diffusion coefficients at reaction conditions, even for a complex reaction system in which the intrinsic kinetics can be well described by a mathematical model. Its application may be limited because the calculations are expensive. To obtain a good estimate of effective diffusion coefficients the reaction conditions must be selected so that no reactants are always in excess.

The concentration distributions of the reactants in catalyst particles show an excess of hydrogen at 80°C or at high HPA conversion. At 60 to 80°C the rates of formation of HPA and PD do not increase significantly when the partial pressure of hydrogen is increased. Instead, the small effective diffusion coefficients of HPA and PD are caused by small micropores of the catalyst particles. Therefore, intraparticle diffusion can be enhanced by enlarging the micropores. Small catalyst particles should be used to enhance the hydrogenation of HPA.

Acknowledgment

Financial support for this work by Deutsche Forschungsgemeinschaft is gratefully acknowledged.

Notation

$\boldsymbol{A}$ = matrix $\boldsymbol{A}$ in Eq. 17
$\boldsymbol{B}$ = matrix $\boldsymbol{B}$ in Eq. 14
$\boldsymbol{D}$ = matrix in Eq. 21
D_{ei} = effective diffusivity of component i, cm^2/s
d_{LL} = diagonal element of the matrix D in Eq. 21
$\boldsymbol{F}$ = vector F in Eq. 15
f_{ij} = defined by Eq. 15
h = step length
H = Henry constant l, MPa/mol
$\boldsymbol{J}$ = matrix in Eq. 23
K = adsorption equilibrium constant of component i, l/mol
n = number of time interval in the numerical integration
P = hydrogen pressure, MPa
r = r-axis in the cylindrical coordinate, cm
R = gas constant, kJ/mol K
R_p = radius of the cylindric catalyst pellets, cm
T = temperature, K or °C
t_α = t-distribution function
$\boldsymbol{U}$ = vector in Eq. 16
u_i = dimensionless concentration of component i, $u_i = C_i/C_{is}$
u_{ij} = dimensionless concentration of component i at point j (Eq. 15)
$\boldsymbol{U}_i$ = vector for component i (Eq. 15)

Greek letters

ϵ_p = porosity of catalyst particle
ρ = dimensionless polar coordinate
ρ_p = density of the catalyst particle, g/L
η_{ie} = apparent effectiveness factors of component i ($i = H_2$, HPA, PD) as determined from experiments

Literature Cited

Arntz, D., Th. Haas, A. Müller, and N. Wiegand, "Kinetische Untersuchung zur Hydratisierung von Acrolein," *Chem. Ing. Tech.*, **63**, 733 (1991).

Haag, W. O., R. M. Logo, and P. B. Weisz, "Transport and Reactivity of Hydrocarbon Molecules in a Shape-Selective Zeolite," *Faraday Discuss.*, **72**, 317 (1981).

Kärger, J., and D. M. Ruthven, *Diffusion in Zeolites and other Microporous Solids*, Wiley, New York (1986).

Kawakami, K., S. Ura, and K. Kusunoki, "The Effectiveness Factor of a Catalyst Pellet in the Liquid-Phase Hydrogenation of Styrene," *J. Chem. Eng. Japan*, **9**, 392 (1976).

Kenney, C. N., and W. Sedriks, "Effectiveness Factor in Three-Phase Slurry Reactor Hydrogenation of Crotonaldehyde," *Chem. Eng. Sci.*, **27**, 2029 (1972).

Lemcoff, N. O., and G. J. Jameson, "Hydrogenation of Acetone in a Vibrating Slurry Reactor," *AIChE J.*, **21**, 730 (1975).

Pfeifer, H., "Surface Phenomena Investigation by Nuclear Magnetic Resonance," *Phys. Rep. (Phys. Lett. C)*, **26**, 293 (1976).

Ruthven, D. M., *Principles of Adsorption and Adsorption Processes*, Wiley, New York (1984).
Satterfield, C. N., A. A. Pelossof, and T. K. Sherwood, "Mass Transfer Limitations in a Trickle-Bed Reactor," *AIChE J.*, **15**, 226 (1969).
Satterfield, C. N., W. J. Ma, and T. K. Sherwood, "The Effectiveness Factor in a Liquid-Filled Porous Catalyst," *AIChE Symp. Ser.*, No. 28 (1968).
Shah, D. B., and D. M. Ruthven, "Measurement of Zeolitic Diffusivities and Equilibrium Isotherms by Chromatography," *AIChE J.*, **23**, 804 (1977).
Turek, F., R. K. Chakrabarti, R. Lange, R. Geik, and W. Flock, "Hydrogenation of Glucose on Nickel Catalyst," *Chem. Eng. Sci.*, **38**, 275 (1983).
Turek, F., and H. Winter, "Drehkorbreaktoren zur experimentellen Untersuchung katalytischer Gas-Flüssig-Reaktionen," *Chem. Tech.*, **42**, 252 (1990).
Wicke, E., and R. Kallenbach, "Die Oberflächendiffusion von Kohlendioxid in aktiven Kohlen," *Kolloid-Z.*, **97**, 135 (1941).
Unruh, J. D., D. A. Ryan, and I. Nicolau, "Method for the Manufacture of 1.3-Propanediol," U.S. Patent 5,093,537 (1992).
Zhu, X. D., "Untersuchungen zum Scale-up von Rieselreaktoren am Beispiel der Hydrierung von 3-Hydroxypropanal," PhD Thesis, Univ. of Erlangen-Nürnberg (1995).
Zhu, X. D., G. Valerius, H. Hofmann, Th. Haas, and D. Arntz, "Intrinsic Kinetics of 3-Hydroxypropanal Hydrogenation over $Ni/SiO_2/Al_2O_3$ Catalyst," *Ind. Eng. Chem. Res.*, accepted (1996a).
Zhu, X. D., Valerius, G., and H. Hofmann, "Effective Kinetics of 3-Hydroxypropanal Hydrogenation over $Ni/SiO_2/Al_2O_3$ Catalyst," *Chem. Eng. Proc.*, accepted (1996b).

Manuscript received Mar. 29, 1996, and revision received July 29, 1996.